

# **Effect of the preparation conditions on the catalytic activity of calcined Ca/Al-layered double hydroxides for the synthesis of glycerol carbonate**

**Judith Granados-Reyes, Pilar Salagre, Yolanda Cesteros\***

Departament de Química Física i Inorgànica. Universitat Rovira i Virgili.

C/ Marcel·lí Domingo s/n, 43007 Tarragona, Spain.

## **Abstract**

The effect of the preparation conditions of several calcined Ca/Al layered double hydroxide compounds (CaAl-LDH) on the catalytic transesterification of glycerol with dimethyl carbonate to obtain glycerol carbonate has been studied. The CaAl-LDH precursors were prepared by aging under microwaves or conventional heating, and using chlorides or nitrates as interlayer anions. Calcination conditions, such as temperature, time and calcination system, were modified. After 3 h of reaction, the catalysts obtained by calcination at 450 °C for 15 h in air exhibited moderate-high glycerol conversion (46-76%) and moderate selectivity to glycerol carbonate (41-65%). Calcination at 450 °C at longer calcination time or the use of a dynamic inert-atmosphere system during calcination led to higher conversion (89-94%) and higher selectivity to glycerol carbonate (72-73%). This has been related to the higher basicity of these catalysts. Finally, calcination at 750 °C resulted in high conversion (88-98%) and high selectivity to glycerol carbonate (60-85%) due to the presence in the catalysts of highly basic CaO. Several catalytic reuses favoured the decarboxylation of glycerol carbonate resulting in the formation of higher amounts of glycidol (42%). The progressive loss of conversion and selectivity to glycerol carbonate observed has been attributed to the loss of some CaO basic centres during reaction.

Keywords: Calcined CaAl-LDH; Glycerol; Glycerol carbonate; calcination conditions.

## 1. Introduction

During biodiesel production, by transesterification of vegetable oils with methanol, glycerol (glycerine or 1,2,3-propanotriol) is formed as by-product in high amounts (10 wt% of the total product). The price of glycerol is falling as fast as biodiesel plants are being built. Research is currently starting to find new outlets to convert the surplus of glycerol into high-added value products that improve the economy of the whole process [1–6].

Glycerol carbonate (4-hydroxymethyl-1,3-dioxolan-2-one) is one of the most attractive glycerol derivatives due to its low toxicity, good biodegradability and high boiling point [7]. This compound has many applications in different industrial sectors, such as intermediate in polymer synthesis [3, 8], biolubricant owing to its adhesion to metallic surfaces and resistance to oxidation, hydrolysis, and pressure [1], protector in the carbohydrates chemistry, component of gas separation membranes, in coatings, or in the production of polyurethane foams [9], and surfactants [10]. Glycerol carbonate could also serve as a source of glycidol, which is employed in textile, plastics, pharmaceutical and cosmetics industries [11]. Traditionally, glycerol carbonate has been industrially produced by reacting glycerol with phosgene but due to the high toxicity and corrosive nature of this reagent, new routes have been investigated [7].

One alternative option consists of obtaining glycerol carbonate by the catalytic transesterification reaction of glycerol with organic cyclic carbonates (ethylene carbonate or propene carbonate) or with non-cyclic carbonates (diethyl carbonate or dimethyl carbonate) [7, 12–20]. Dimethyl carbonate is preferred since the reaction can be performed at milder conditions and the co-product methanol can be easily separated.

Biocatalysts have been used in the transesterification reaction of glycerol with dimethyl carbonate to obtain glycerol carbonate. However, this method need long reaction times [21,22]. Some studies have been carried out using zeolites as catalysts for the transesterification reaction of glycerol with dimethyl carbonate [23–25]. Additionally, Ochoa-Gomez et al. [12] studied different reaction conditions with different basic and acid homogeneous and heterogeneous catalysts. The best results were achieved using a basic heterogeneous catalyst (CaO). The CaO showed 100% of conversion and >95% yield after 1.5 h of reaction at 95 °C. However, when reused, CaO deactivated due to the contact with air between catalytic runs, and because of particle agglomeration [12].

Hydrotalcite-based catalysts have been widely employed for the transesterification reaction; Alvarez et al. [26] used MgAl hydrotalcites supported on  $\alpha$ - and  $\gamma$ -Al<sub>2</sub>O<sub>3</sub>, and also prepared hydrotalcite-like compounds containing a Mg/Al molar ratio of 4, activated by calcination, followed by rehydration under ultrasounds [27], or by anion exchange (F<sup>-</sup>, Cl<sup>-</sup>, CO<sub>3</sub><sup>2-</sup>) [28]. Also Zheng et al. [29] studied this reaction using MgAl hydrotalcites with different Mg/Al ratios. The sample with ratio equal to 2 showed 97% of selectivity to GC and 67% of glycerol conversion at 70 °C for 3 h. Yadav et al. [20] studied the effects of various hydrotalcites with different Mg/Al composition loaded on hexagonal mesoporous silica for this reaction of glycerol, in autoclave at 230 °C for 3 h. They obtained a glycerol conversion of 85% and selectivity to glycerol carbonate between 84-88%. Other authors have studied this reaction with ZnO/La<sub>2</sub>O<sub>3</sub> mixed oxides [30], Mg/Al/Zr calcined at different temperatures [16], and Mg/Zr/Sr mixed oxide base catalysts [17].

Hydrocalumite-type compounds belong to the layered double hydroxides family (LDHs) with formula  $[M(II)_{1-x}M(III)_x(OH)_2][X^{q-}_{x/q} \cdot nH_2O]$  where  $[Ca_2Al(OH)_6]^+$  represents the hydrocalumite layer composition, and  $[X^{q-}_{x/q} \cdot nH_2O]$  the interlayer composition [31].

Especially, the hydrocalumite name is used when the interlayer anion is chloride. The CaAl-LDH structure collapses at temperatures between 400 °C and 600 °C resulting in the formation of amorphous mixed oxides, Ca(Al)O<sub>x</sub>. At higher calcination temperatures crystalline CaO and mayenite (Ca<sub>12</sub>Al<sub>14</sub>O<sub>33</sub>) phases are obtained. These basic mixed oxides have been scarcely used as catalysts for aldol condensation, Meerwein-Ponndorf-Verley or isomerization of 1-butene reactions [32–34].

The aim of this work was to study the effect of the preparation conditions of several calcined Ca/Al hydrocalumite-type compounds on the catalytic transesterification of glycerol with dimethyl carbonate to obtain glycerol carbonate [35]. The CaAl-LDH precursors have been prepared by aging under microwaves or conventional heating, and using chlorides or nitrates as interlayer anions. Calcination conditions, such as temperature, time and calcination system, have been modified.

## **2. Material and methods**

### *2.1. Samples preparation*

Ten CaAl-LDH samples were synthesized by the co-precipitation method from different starting salts under vigorous magnetic stirring using deionized/decarbonated water, as well as nitrogen atmosphere. Two aqueous solutions containing CaCl<sub>2</sub>·2H<sub>2</sub>O (sigma-Aldrich, ≥ 99 %) and AlCl<sub>3</sub>·6H<sub>2</sub>O (Riedel-de Haën, ≥ 99 %) (series HC1) or Ca(NO<sub>3</sub>)<sub>2</sub>·4H<sub>2</sub>O (sigma-Aldrich, ≥ 99 %) and Al(NO<sub>3</sub>)<sub>3</sub>·9H<sub>2</sub>O (sigma-Aldrich, ≥ 98 %) (series HC2), were prepared with a 2:1 Ca<sup>2+</sup>/Al<sup>3+</sup> molar ratio by adding an aqueous solution of 2 M NaOH (Panreac, QP) at 60 °C and constant pH of 11.5 [36]. After complete addition of the metallic salts, the two mother solutions were aged by several treatments: by refluxing in conventional heating at 60 °C for 24 h (HC1R<sub>24</sub> and HC2R<sub>24</sub>), by refluxing under microwaves (Milestone ETHOS-TOUCH CONTROL, 2.45 GHz)

with a power of 400 W at 60 °C for 6 h (HC1RM<sub>w6</sub> and HC2RM<sub>w6</sub>), in autoclave by conventional heating at 180 °C for 1 h (HC1AC<sub>1</sub> and HC2AC<sub>1</sub>), and in autoclave under microwaves at 180 °C for 1 h (HC1AM<sub>w1</sub> and HC2AM<sub>w1</sub>) and for 3 h (HC1AM<sub>w3</sub> and HC2AM<sub>w3</sub>) (microwaves power of 600 W). All samples were filtered at room temperature, washed with deionized and decarbonated water and then dried in an oven at 80 °C overnight.

For the preparation of the catalysts, all the hydrocalumite-type compounds were calcined in a furnace Carbolite CWF11/5P8 at 450 °C for 15 h (cHC1R<sub>24</sub>, cHC2R<sub>24</sub>, cHC1RM<sub>w6</sub>, cHC2RM<sub>w6</sub>, cHC1AC<sub>1</sub>, cHC2AC<sub>1</sub>, cHC1AM<sub>w1</sub>, cHC2AM<sub>w1</sub>, cHC1AM<sub>w3</sub>, cHC2AM<sub>w3</sub>). To determine the influence of the calcination time, and the effect of using a dynamic inert atmosphere system during calcination, one of the CaAl-LDH samples (HC1AM<sub>w3</sub>) was calcined 450 °C for 24 h (cHC1AM<sub>w3-24h</sub>), and other sample by flowing nitrogen gas (1 mL/s) at 450 °C for 10 h in a quartz reactor (cHC1AM<sub>w3-N<sub>2</sub></sub>). Finally, in order to study the effect of the calcination temperature, several samples were calcined at 750 °C for 4 h (cHC1AC<sub>1-750</sub>, cHC1AM<sub>w1-750</sub>, cHC1AM<sub>w3-750</sub>, cHC2AC<sub>1-750</sub> and cHC2AM<sub>w1-750</sub>). Table 1 summarizes the preparation conditions of all samples.

## 2.2. X-ray diffraction (XRD)

Powder X-ray diffraction patterns of the calcined samples were obtained with a Siemens D5000 diffractometer using nickel-filtered CuK $\alpha$  radiation and detecting between 2 $\theta$  values of 5°-70°. Crystalline phases were identified using the Joint Committee on Powder Diffraction Standards (JCPDS) files (086-2340- calcite, 048-1882-mayenite, 037-1497-lime).

### *2.3. Elemental Analysis*

Elemental analysis of the hydrocalumite-type compounds was obtained with an ICP-OES analyser (Induced Coupled Plasma–Optical Emission Spectroscopy) from Spectro Arcos. The digestion of all samples was carried out with concentrated HNO<sub>3</sub>. Analyses were performed by triplicate.

### *2.4. Nitrogen Physisorption*

BET surface areas were calculated from the nitrogen adsorption isotherms at -196 °C using a Quantachrome Quadrasorb SI surface analyzer and a value of 0.164 nm<sup>2</sup> for the cross-section of the nitrogen molecule. Samples were degassed at 90 °C.

### *2.5. Scanning electron microscopy (SEM)*

Scanning electron micrographs were obtained with a JEOL JSM-35 C scanning microscope operating at an accelerating voltage in the range 15-30 kV, work distance of 14 mm and magnification values between 5000 and 30000x.

### *2.6. Transmission electron microscopy (TEM)*

Transmission electron microscopy of the samples was performed using a JEOL electron microscope Model 1011 with an operating voltage of 80 kV. Samples were dispersed in acetone and a drop of the suspension was poured on to a carbon coated cooper grip and dried at room temperature before measurements. The magnification values used were between 20 and 100 k.

### *2.7. Hammett's indicators*

Basicity of the catalysts was evaluated using Hammett's indicators: phenolphthalein (pKa = 8.2), nile blue A (pKa = 10.1), tropaeolin O (pKa = 11), thiazole yellow G (pKa = 13.4) and 2,4-dinitroaniline (pKa = 15). 25 mg of catalyst was taken along with 2.5 mL dry methanol and 1 mL of indicator, and kept in a shaker for 2 h.

## 2.8. Catalytic Tests

For the catalytic tests, dimethyl carbonate (Sigma Aldrich, 99 %) and glycerol (Sigma-Aldrich,  $\geq 99$  %) were mixed in a 3.5:1 weight ratio in a 50 mL round bottom 3-neck jacketed glass reactor fitted with a magnetic stirrer, a reflux condenser and a thermometer. The reaction was solvent-free. The mixture was heated at 90 °C with constant stirring at 1000 rpm under N<sub>2</sub>. Then, 0.15 g of catalyst was added to start the reaction. After 3 h of reaction, the mixture was filtered and evaporated in a rotatory evaporator. 1  $\mu$ L of the concentrated residue was analysed by gas chromatography. The reaction conditions (catalyst loading, speed of agitation, reaction temperature and reaction time) were previously optimized. Regarding the fine powder used (particle size below 5  $\mu$ m), the high speed of agitation, and the absence of microporosity in the catalysts, external and internal diffusion problems should be neglected.

Gas chromatography analyses were performed in a Shimadzu GC-2010 apparatus, equipped with a split injection mode and a flame ionization detector. The column was a 60 m length SUPRAWAX-280 with a film thickness of 50  $\mu$ m and an internal diameter of 0.25 mm. The “Split” injection mode was selected with a 20/1 separation ratio. The carrier gas was helium. The temperature of the injector and detector was set to 250 °C. The temperature programme of the oven started at 120 °C during 3 minutes followed by a ramp of 15 °C/min until reaching 200 °C. Next, the temperature was increased at 20 °C/min until 250 °C and was held at this temperature for 30 min.

Glycerol conversion and selectivity to glycerol carbonate and glycidol were determined from calibration lines obtained from commercial products.

Conversion and selectivity values of the catalytic tests were calculated according to the following equations:

$$\text{Conversion (\%)} = \frac{\text{moles of glycerol converted}}{\text{moles of initial glycerol}} \times 100$$

$$\text{Selectivity to product x (\%)} = \frac{\text{moles of glycerol converted to product x}}{\text{moles of converted glycerol}} \times 100$$

### 3. Results and discussion

#### 3.1. X-ray diffraction (XRD)

XRD patterns of the cHC1 samples, prepared from chloride salts and calcined at 450 °C for 15 h, mainly showed the presence of an amorphous phase due to the expected mixture of calcium and aluminium oxides,  $\text{Ca(Al)O}_x$  (Figure 1a-e). Additionally, several crystalline peaks were observed for most of the samples (cHC1AC<sub>1</sub>, cHC1RMw<sub>6</sub>, cHC1AMw<sub>1</sub> and cHC1AMw<sub>3</sub>) that were identified as calcite ( $\text{CaCO}_3$ ). The presence of the calcite phase can be related to the air atmosphere used during calcination. By increasing the calcination time in air, from 15 to 24 h, the calcite content increased and new crystalline peaks, corresponding to the mayenite phase,  $\text{Ca}_{12}\text{Al}_{14}\text{O}_{33}$  appeared (Figure 1f). The use of nitrogen flowing through the sample during calcination for 10 h favoured the crystallization of mayenite and a small amount of CaO was observed (Figure 1g), this could be associated with the easier elimination of the gases generated during calcination in this dynamic system. Additionally, calcite was also observed in low amounts. Some  $\text{CO}_2$  formed during calcination could react with some  $\text{Ca}^{2+}$  to form calcite in this sample. This  $\text{CO}_2$  comes from carbonates located as interlayer anions in the starting hydrocalumite.

XRD patterns of the cHC2 samples, prepared from nitrate salts and calcined at 450 °C for 15 h, are shown in Figure 2. cHC2 samples were more crystalline than cHC1 samples

(Figure 1). The cHC2 samples aged under reflux only exhibited crystalline peaks corresponding to the calcite phase (Figure 2a and 2b) whereas the cHC2 samples aged in autoclave showed, in addition to lower amounts of calcite, the presence of the mayenite phase, which was more crystalline for the sample aged under microwaves at longer time (Figure 2e). Therefore, the use of nitrate anions for the preparation of hydrocalumite-type compounds favoured the formation, after calcination, of the mayenite phase when using autoclave-aging conditions, especially under microwaves.

Several Ca/Al LDHs were calcined at higher temperature (750 °C for 4 h). A mixture of CaO and mayenite phase was obtained in all cases (Figure 3). These samples did not show the calcite phase since this compound decomposes at lower temperature than the calcination temperature used. The samples obtained from chloride salts and aged under microwaves exhibited, after calcination at these conditions, higher amounts of the CaO phase.

### *3.2. Elemental analysis*

Ca/Al molar ratio of cHC1 samples were around 2, in agreement with the Ca/Al molar ratio of the starting solutions used for the coprecipitation of their precursors, except for the sample aged at longer time in autoclave with microwaves (cHC1AMw<sub>3</sub>), which had slight higher Ca/Al molar ratio (Table 2). Longer aging times in autoclave with microwaves could involve some dealumination of the hydrocalumite layers, explaining the higher Ca/Al molar ratio of cHC1AMw<sub>3</sub>. This effect was previously observed in the preparation of hydrotalcites with microwaves [37]. Ca/Al molar ratio values of the samples whose precursors were prepared from nitrates (cHC2) were lower than those obtained from the samples synthesized with chloride salts (cHC1) (Table 2). This has been related to the presence in their precursors of different amounts of katoite phase

(Ca<sub>3</sub>Al<sub>2</sub>(OH)<sub>12</sub>) [36], which has a Ca/Al ratio of 1.5. Thus, cHC2AMw<sub>3</sub>, whose precursor had the highest amount of katoite, showed the lowest Ca/Al ratio (Table 2).

### 3.3. Nitrogen physisorption

All calcined samples presented nitrogen adsorption-desorption isotherms of type IV, which according to the IUPAC classification corresponded to mesoporous solids with pore size distribution in the mesoporous range (20-500 Å).

Table 2 shows the surface area, average pore size and pore volume values obtained for all samples. Calcined Ca/Al LDHs had low surface areas in the range 4-13 m<sup>2</sup>/g (Table 2). This agrees with the results reported by other authors for calcined hydrocalumite-type compounds [34, 38]. Regarding the surface areas of the samples calcined at 450 °C, we observe that cHC1 samples exhibited slight higher surface areas than cHC2 samples. This can be related to the lower crystallinity observed by XRD for cHC1 samples (Figure 1). After calcination at higher temperature (750 °C), a decrease of surface area was observed, as expected, due to the presence of CaO and mayenite phases with higher crystallinity (Figure 3).

### 3.4. Scanning electron microscopy (SEM) and Transmission electron microscopy (TEM)

Figure 4 shows some representative SEM and TEM images of the samples. SEM allowed us to observe that calcined samples retained the original hexagonal morphology of their precursors, the hydrocalumite-type compounds [36]. This means that despite the thermal decomposition and the consequent changes suffered by the structure due to the loss of water, anions and dehydroxilation processes, there were not significant changes in the crystal morphology of the particles. Samples calcined at 750 °C showed a greater deformation of the edges, more compact and more agglomerated particles than those calcined at 450 °C, explaining their lower surface areas.

TEM images also confirmed the presence of hexagonal sheets, but not so well differentiated as in their precursors [36] and more compacted, probably because of the water release and crystallographic phase transformation. This would also account for the low specific surface areas measured for the calcined solids (Table 2).

### 3.5. *Hammett's indicators*

Hammett's indicators results showed that all the samples calcined at 450 °C for 15 h in air had the same basicity ( $6.8 < H_- < 8.2$ ) (Table 2). However, the sample calcined at higher calcination time, cHC1AMw<sub>3</sub>-24, showed higher basicity strength ( $8.2 < H_- < 10.1$ ), probably due to the presence of mayenite phase in this sample, and the sample calcined in an inert atmosphere in a dynamic system, cHC1AMw<sub>3</sub>-N<sub>2</sub>, exhibited the highest basicity strength ( $10.1 < H_- < 13.4$ ) regarding the samples calcined at 450 °C. This could be attributed to the presence of a low amounts of CaO (known for its basicity), and lower amounts of calcite phase. The presence of higher amounts of more crystalline calcite in the samples calcined at 450 °C for 15 h in air could justify the lower basicity of these samples. The use of higher calcination time or an inert atmosphere could reduce the formation of this calcite phase, and therefore higher basicity was obtained. Finally, the stronger basicity observed for the samples calcined at 750 °C ( $13.4 < H_- < 15$ ) can be related to the presence of CaO, highly basic, together with the absence of calcite, which decomposed at these higher calcination temperatures.

### 3.6. *Catalytic Activity*

Figure 5 and 6 show the catalytic results obtained by using the cHC1 and cHC2 catalysts prepared by calcination at 450 °C for the transesterification of glycerol with dimethyl carbonate after 3 h of reaction. All the catalysts calcined at the same conditions (cHC1R<sub>24</sub>, cHC2R<sub>24</sub>, cHC1RMw<sub>6</sub>, cHC2RMw<sub>6</sub>, cHC1AC<sub>1</sub>, cHC2AC<sub>1</sub>, cHC1AMw<sub>1</sub>, cHC2AMw<sub>1</sub>,

cHC1AMw<sub>3</sub>, cHC2AMw<sub>3</sub>) exhibited moderate-high glycerol conversion (46-76%) and moderate selectivity to glycerol carbonate (41-65%).

Conversion and selectivity values to glycerol carbonate were slightly higher for the catalysts whose precursors were aged under microwaves by refluxing as well as autoclave. This could be correlated with the higher amounts of calcite observed for these catalysts, which neutralizes the strongest basic centers responsible for the deactivation. Interestingly, the two catalysts calcined at 450 °C but at longer calcination time (cHC1AMw<sub>3</sub>-24h) or using a dynamic inert-atmosphere system during calcination (cHC1AMw<sub>3</sub>-N<sub>2</sub>) led to higher conversion (89-94%) and higher selectivity to glycerol carbonate (72-73%) values than cHC1AMw<sub>3</sub>. The presence of mayenite and calcite with low crystallinity together with the mixed oxide Ca(Al)O<sub>x</sub> (Figure 1), only observed in these two catalysts, could justify these results together with the higher basicity observed in these two catalysts. These results are very interesting taking into account the low surface area of these catalysts, and the lower reaction time used. Additionally, glycidol was detected for all catalysts in different amounts (4-20%). The formation of glycidol during this reaction, by decarboxylation of glycerol carbonate, has been previously reported by other authors over catalysts with high basicity strength [19]. No other reaction products were detected by gas chromatography at the conditions used. The formation of condensation products from glycerol or glycidol could round off the total products obtained.

Figure 7 shows the catalytic activity results of the catalysts calcined at 750 °C. These samples had much higher conversion (88-98%) and much higher selectivity to glycerol carbonate (60-85%) than their corresponding catalysts calcined at 450 °C, especially catalysts cHC1. This can be related to the higher basicity of the catalysts calcined at 750 °C with respect to those calcined at 450 °C, as confirmed by the results obtained by using

Hammett's indicators (Table 2). The higher amounts of CaO, highly basic, detected in cHC1 catalysts (Figure 3) could explain the differences observed between cHC1 and cHC2 catalysts (Figure 7). The results obtained were compared with commercial CaO (Sigma Aldrich, 99.9 %, calcined at 750 °C for 4 h) tested under the same reaction conditions than the catalysts discussed above. CaO showed a glycerol conversion of 77%, selectivity of glycerol carbonate of 87% and selectivity to glycidol of 7%.

Finally, the catalytic life of one of the catalysts (cHC1AM<sub>w1</sub>-750) was evaluated from four consecutive runs performed reusing the catalyst at the same reaction conditions used for the first catalytic test. After each catalytic run, recovering of the catalyst was performed by filtration, mild-washing in methanol at room temperature and dried before reaction. Several catalytic reuses favoured the decarboxylation of glycerol carbonate resulting in the formation of higher amounts of glycidol with a progressive loss of conversion and glycerol carbonate selectivity. This behaviour was previously observed for their hydrotaculamite-type precursors [39] but with these calcined hydrocalumites the formation of glycidol was more marked arriving to 42% after 4 reuses (Figure 8).

By comparing the XRD pattern of the reused catalyst with that of its corresponding fresh catalyst (Figure 9), we observed a decrease in the crystallinity of the mayenite phase and the disappearance of CaO accompanied by the formation of some hydrocalumite in low amounts for the reused sample. Thus, the progressive loss of conversion and selectivity to glycerol carbonate observed could be attributed to the loss of some CaO basic centres during reaction.

From all these results, we can conclude that our calcined Ca/Al LDH catalysts were more stable with time than that reported for CaO catalysts [12]. This could be related to the

presence of mayenite surrounding CaO that could make this CaO less reactant to air than the CaO alone.

#### **4. Conclusions**

CaAl-LDH samples obtained from chloride salts and calcined at 450 °C for 15 h mainly showed the presence of an amorphous  $\text{Ca}(\text{Al})\text{O}_x$  phase together with some calcite ( $\text{CaCO}_3$ ) in most of them. By increasing the calcination time, the calcite content increased and mayenite ( $\text{Ca}_{12}\text{Al}_{14}\text{O}_{33}$ ) appeared. The use of nitrogen flowing through the sample during calcination favoured the crystallization of mayenite. The use of nitrate anions for the preparation of hydrocalumite-type compounds favoured the formation, after calcination, of the mayenite phase when using autoclave-aging conditions, especially under microwaves. For the samples calcined at 750 °C for 4 h, a mixture of CaO and mayenite phase was obtained. All catalysts showed low surface areas (4-13  $\text{m}^2/\text{g}$ ) and retained the original hexagonal morphology of their precursors, the hydrocalumite-type compounds, as observed by SEM and TEM. The basicity strength was higher for the samples calcined at higher temperature, as determined by using Hammet indicators.

The catalysts obtained by calcination at 450 °C for 15 h in air showed moderate-high glycerol conversion (46-76%) and moderate selectivity to glycerol carbonate (41-65%) after 3 h of reaction. The use of longer calcination time at 450 °C or a dynamic inert-atmosphere system during calcination led to higher conversion (89-94%) and higher selectivity to glycerol carbonate (72-73%) values. This has been related to the presence of mayenite and calcite with low crystallinity together with the mixed oxide  $\text{Ca}(\text{Al})\text{O}_x$  in these two catalysts, which had higher basicity strength than the catalysts calcined at 450 °C for 15 h. Calcination at 750 °C resulted in high conversion (88-98%) and high selectivity to glycerol carbonate (60-85%) due to the presence in the catalysts of CaO, highly basic. The progressive loss of conversion and selectivity to glycerol carbonate

observed after several reuses has been attributed to the loss of some CaO basic centres during reaction, resulting in the formation of higher amounts of glycidol (42%).

### **Acknowledgements**

Authors acknowledge Ministerio de Economía y Competitividad of Spain and Feder Funds (CTQ2011-24610), and Catalan Government for FI grant (2012FI\_B00564).

## References

- [1] M. Pagliaro, R. Ciriminna, H. Kimura, M. Rossi, C. Della Pina, *Angew. Chemie Int. Ed.* 46 (2007) 4434–4440.
- [2] R. D'Aquino, G. Ondrey, *Chem. Eng.* 114 (2007) 31–37.
- [3] A. Behr, J. Eilting, K. Irawadi, J. Leschinski, F. Lindner, *Green Chem.* 10 (2008) 13.
- [4] J. Barrault, F. Jerome, *Eur. J. Lipid Sci. Technol.* 110 (2008) 825–830.
- [5] M. Pagliaro, R. Ciriminna, H. Kimura, M. Rossi, C. Della Pina, *Eur. J. Lipid Sci. Technol.* 111 (2009) 788–799.
- [6] N. Rahmat, A.Z. Abdullah, A.R. Mohamed, *Renew. Sustain. Energy Rev.* 14 (2010) 987–1000.
- [7] W.K. Teng, G.C. Ngoh, R. Yusoff, M.K. Aroua, *Energy Convers. Manag.* 88 (2014) 484–497.
- [8] C.-H.C. Zhou, J.N. Beltramini, Y.-X. Fan, G.Q.M. Lu, *Chem. Soc. Rev.* 37 (2008) 527–49.
- [9] D. Randall, R. De Vos, EP 419114, 1991.
- [10] M. Weuthen, U. Hees, DE 4335947, 1995.
- [11] J.W. Yoo, Z. Mouloungui, A. Gaset, US 6316641, 2001.
- [12] J.R. Ochoa-Gómez, O. Gómez-Jiménez-Aberasturi, B. Maestro-Madurga, A. Pesquera-Rodríguez, C. Ramírez-López, L. Lorenzo-Ibarreta, J. Torrecilla-Soria, M.C. Villarán-Velasco, *Appl. Catal. A Gen.* 366 (2009) 315–324.
- [13] F.S.H. Simanjuntak, T.K. Kim, S.D. Lee, B.S. Ahn, H.S. Kim, H. Lee, *Appl. Catal. A Gen.* 401 (2011) 220–225.
- [14] A. Takagaki, K. Iwatani, S. Nishimura, K. Ebitani, *Green Chem.* 12 (2010) 578.
- [15] A. Kumar, K. Iwatani, S. Nishimura, A. Takagaki, K. Ebitani, *Catal. Today.* 185 (2012) 241–246.
- [16] M. Malyaadri, K. Jagadeeswaraiyah, P.S. Sai Prasad, N. Lingaiah, *Appl. Catal. A Gen.* 401 (2011) 153–157.
- [17] G. Parameswaram, M. Srinivas, B.H. Babu, P.S.S. Prasad, N. Lingaiah, *Catal. Sci. Technol.* 3 (2013) 3242–3249.
- [18] P. Liu, M. Derchi, E.J.M. Hensen, *Appl. Catal. B Environ.* 144 (2014) 135–143.

- [19] Z. Liu, J. Wang, M. Kang, N. Yin, X. Wang, Y. Tan, Y. Zhu, *J. Ind. Eng. Chem.* 21 (2015) 394–399.
- [20] G.D. Yadav, P.A. Chandan, *Catal. Today.* 237 (2014) 47–53.
- [21] Y.J. Jo, O.K. Lee, E.Y. Lee, *Bioresour. Technol.* 158 (2014) 105–10.
- [22] G. V Waghmare, M.D. Vetel, V.K. Rathod, *Ultrason. Sonochem.* 22 (2015) 311–6.
- [23] Y.T. Algoufi, B.H. Hameed, *Fuel Process. Technol.* 126 (2014) 5–11.
- [24] S. Pan, L. Zheng, R. Nie, S. Xia, P. Chen, Z. Hou, *Chinese J. Catal.* 33 (2012) 1772–1777.
- [25] J. Hu, Y. Gu, Z. Guan, J. Li, W. Mo, T. Li, G. Li, *ChemSusChem.* 4 (2011) 1767–72.
- [26] M.G. Álvarez, M. Plíšková, A.M. Segarra, F. Medina, F. Figueras, *Appl. Catal. B Environ.* 113-114 (2012) 212–220.
- [27] M.G. Álvarez, A.M. Segarra, S. Contreras, J.E. Sueiras, F. Medina, F. Figueras, *Chem. Eng. J.* 161 (2010) 340–345.
- [28] M.G. Álvarez, R.J. Chimentão, F. Figueras, F. Medina, *Appl. Clay Sci.* 58 (2012) 16–24.
- [29] L. Zheng, S. Xia, Z. Hou, M. Zhang, Z. Hou, *Chinese J. Catal.* 35 (2014) 310–318.
- [30] M. Hong, L. Gao, G. Xiao, *J. Chem. Res.* 38 (2014) 679–681.
- [31] R. Segni, L. Vieille, F. Leroux, C. Taviot-Guého, *J. Phys. Chem. Solids.* 67 (2006) 1037–1042.
- [32] M. Mora, M.I. López, C. Jiménez-Sanchidrián, J.R. Ruiz, *Catal. Letters.* 136 (2010) 192–198.
- [33] I. Cota, E. Ramírez, F. Medina, J.E. Sueiras, G. Layrac, D. Tichit, *Appl. Clay Sci.* 50 (2010) 498–502.
- [34] E. Lopez-Salinas, M.E.L. Serrano, M.A.C. Jacome, I.S. Secora, *J. Porous Mater.* 2 (1996) 291–297.
- [35] J. Granados-Reyes. Hydrocalumite-based catalysts for glycerol revalorization. PhD thesis, 2015.
- [36] J. Granados-Reyes, P. Salagre, Y. Cesteros, *Micropor. Mesopor. Mater.* 199 (2014) 117–124.

- [37] O. Bergadà, I. Vicente, P. Salagre, Y. Cesteros, F. Medina, J.E. Sueiras, *Micropor. Mesopor. Mater.* 101 (2007) 363–373.
- [38] C.F. Linares, F. Ocanto, P. Bretto, M. Monsalve, *Bull. Mater. Sci.* 37 (2014) 941–944
- [39] J. Granados-Reyes, P. Salagre, Y. Cesteros, *Appl. Clay Sci.* (2016)

**Table 1.**

Sample*	Aging conditions of the precursors				Calcination		
	Heating	Technique	T (°C)	Time (h)	T (°C)	Time (h)	System
cHC1R <sub>24</sub>	conventional	refluxing	60	24	450	15	static/air
cHC1RM <sub>w6</sub>	microwave	refluxing	60	6	450	15	static/air
cHC1AC <sub>1</sub>	conventional	autoclave	180	1	450	15	static/air
cHC1AM <sub>w1</sub>	microwave	autoclave	180	1	450	15	static/air
cHC1AM <sub>w3</sub>	microwave	autoclave	180	3	450	15	static/air
cHC1AM <sub>w3-24</sub>	microwave	autoclave	180	3	450	24	static/air
cHC1AM <sub>w3-N<sub>2</sub></sub>	microwave	autoclave	180	3	450	10	dynamic/N <sub>2</sub>
cHC2R <sub>24</sub>	conventional	refluxing	60	24	450	15	static/air
cHC2RM <sub>w6</sub>	microwave	refluxing	60	6	450	15	static/air
cHC2AC <sub>1</sub>	conventional	autoclave	180	1	450	15	static/air
cHC2AM <sub>w1</sub>	microwave	autoclave	180	1	450	15	static/air
cHC2AM <sub>w3</sub>	microwave	autoclave	180	3	450	15	static/air
cHC1AC <sub>1-750</sub>	conventional	autoclave	180	1	750	4	static/air
cHC1AM <sub>w1-750</sub>	microwave	autoclave	180	1	750	4	static/air
cHC1AM <sub>w3-750</sub>	microwave	autoclave	180	3	750	4	static/air
cHC2AC <sub>1-750</sub>	conventional	autoclave	180	1	750	4	static/air
cHC2AM <sub>w1-750</sub>	microwave	autoclave	180	1	750	4	static/air

\* **HC1:** Chloride salts, **HC2:** Nitrate salts

**Table 2.**

Samples	Ca/Al	Surface Area (m <sup>2</sup> g <sup>-1</sup> )	Average Pore Size (Å)	Pore Volume (cm <sup>3</sup> g <sup>-1</sup> )	Hammett's Indicators
cHC1R <sub>24</sub>	1.98	11	147	0.08	6.8<H_>8.2
cHC1RM <sub>w6</sub>	1.87	12	129	0.07	6.8<H_>8.2
cHC1AC <sub>1</sub>	1.96	11	100	0.05	6.8<H_>8.2
cHC1AM <sub>w1</sub>	1.93	13	160	0.10	6.8<H_>8.2
cHC1AM <sub>w3</sub>	2.12	7	79	0.03	6.8<H_>8.2
cHC1AM <sub>w3-24</sub>	2.12	9	88	0.04	8.2<H_>10.1
cHC1AM <sub>w3-N<sub>2</sub></sub>	2.12	9	104	0.04	10.1<H_>13.4
cHC2R <sub>24</sub>	1.79	9	124	0.05	6.8<H_>8.2
cHC2RM <sub>w6</sub>	1.63	10	86	0.04	6.8<H_>8.2
cHC2AC <sub>1</sub>	1.76	9	96	0.04	6.8<H_>8.2
cHC2AM <sub>w1</sub>	1.42	8	98	0.07	6.8<H_>8.2
cHC2AM <sub>w3</sub>	1.38	4	144	0.03	6.8<H_>8.2
cHC1AC <sub>1-750</sub>	1.96	5	95	0.02	13.4<H_>15
cHC1AM <sub>w1-750</sub>	1.93	4	100	0.02	13.4<H_>15
cHC1AM <sub>w3-750</sub>	2.12	5	128	0.03	13.4<H_>15
cHC2AC <sub>1-750</sub>	1.76	7	103	0.06	13.4<H_>15
cHC2AM <sub>w1-750</sub>	1.42	7	129	0.05	13.4<H_>15

## LEGENDS AND CAPTIONS

**Table 1.** Preparation conditions of calcined CaAl-LDHs.

**Table 2.** Characterization results of the samples.

**Figure 1.** XRD patterns of the samples obtained from chlorides salts a) cHC1R<sub>24</sub>, b) cHC1RM<sub>w6</sub>, c) cHC1AC<sub>1</sub>, d) cHC1AM<sub>w1</sub>, e) cHC1AM<sub>w3</sub>, f) cHC1AM<sub>w3-24</sub>, g) cHC1AM<sub>w3-N<sub>2</sub></sub>. ■ Calcite phase; ■ Mayenite phase ■ CaO phase.

**Figure 2.** XRD patterns of the samples prepared from nitrate salts a) cHC2R<sub>24</sub>, b) cHC2RM<sub>w6</sub>, c), cHC2AC<sub>1</sub> d) cHC2AM<sub>w1</sub>, e) cHC2AM<sub>w3</sub>. ■ Calcite phase; ■ Mayenite phase

**Figure 3.** XRD patterns of the samples a) cHC1AC<sub>1-750</sub>, b) cHC1AM<sub>w1-750</sub>, c) cHC1AM<sub>w3-750</sub>, d) cHC2AC<sub>1-750</sub>, e) cHC2AM<sub>w1-750</sub>. ■ Mayenite phase; ■ CaO phase.

**Figure 4.** SEM images of a) cHC1AC<sub>1</sub> (x20000), b) cHC1AM<sub>w1</sub> (x13000), c) cHC2AC<sub>1</sub> (x8000), d) cHC2AM<sub>w1</sub> (x17000), e) cHC1AC<sub>1-750</sub> (x9500), f) cHC1AM<sub>w1-750</sub> (x12000), g) cHC2AC<sub>1-750</sub> (x20000), h) cHC2AM<sub>w1-750</sub> (x9000), and TEM images of i) cHC1R<sub>24</sub> (x60000), j) cHC1RM<sub>w6</sub> (x80000), k) cHC2R<sub>24</sub> (x50000), l) cHC2RM<sub>w6</sub> (x25000).

**Figure 5.** Catalytic activity results of the cHC1 catalysts obtained by calcination at 450 °C. Reaction conditions: dimethyl carbonate/glycerol = 3.5:1 weight ratio; stirring 1000 rpm; N<sub>2</sub> atmosphere; 0.15 g of catalyst; temperature: 90 °C; time: 3 h.

**Figure 6.** Catalytic activity results of the cHC2 catalysts obtained by calcination at 450 °C. Reaction conditions: dimethyl carbonate/glycerol = 3.5:1 weight ratio; stirring 1000 rpm; N<sub>2</sub> atmosphere; 0.15 g of catalyst; temperature: 90 °C; time: 3 h.

**Figure 7.** Catalytic activity results of several catalysts calcined at 750 °C. Reaction conditions: dimethyl carbonate/glycerol = 3.5:1 weight ratio; stirring 1000 rpm; N<sub>2</sub> atmosphere; 0.15 g of catalyst; temperature: 90 °C; time: 3 h.

**Figure 8.** Reuse studies of catalyst cHC1AM<sub>w1-750</sub>. Reaction conditions: dimethyl carbonate/glycerol = 3.5:1 weight ratio; stirring 1000 rpm; N<sub>2</sub> atmosphere; 0.15 g of catalyst; temperature: 90 °C; time: 3 h

**Figure 9.** XRD patterns of the catalyst cHC1AM<sub>w1-750</sub>: a) fresh catalyst and b) after reaction. Reaction conditions: dimethyl carbonate/glycerol = 3.5:1 weight ratio; stirring 1000 rpm; N<sub>2</sub> atmosphere; 0.15 g of catalyst; temperature: 90 °C; time: 3 h. ■ Mayenite phase; ■ CaO phase; ■ Hydrocalumite phase.

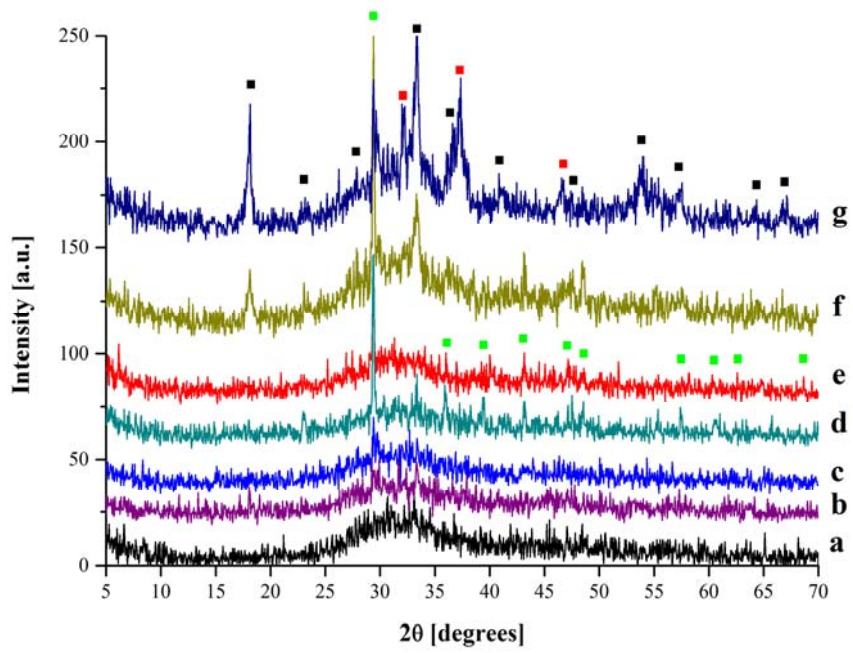


Figure 1.

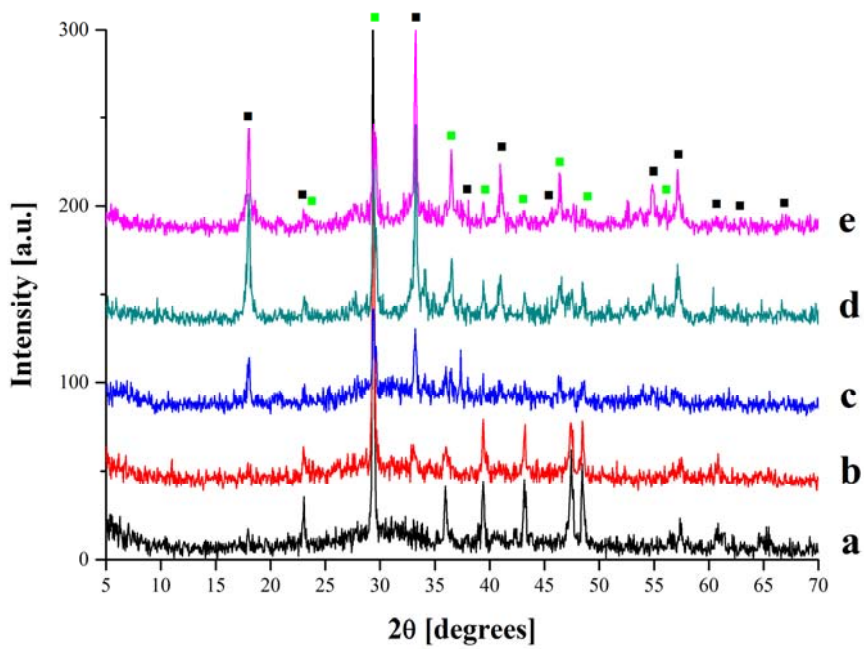


Figure 2.

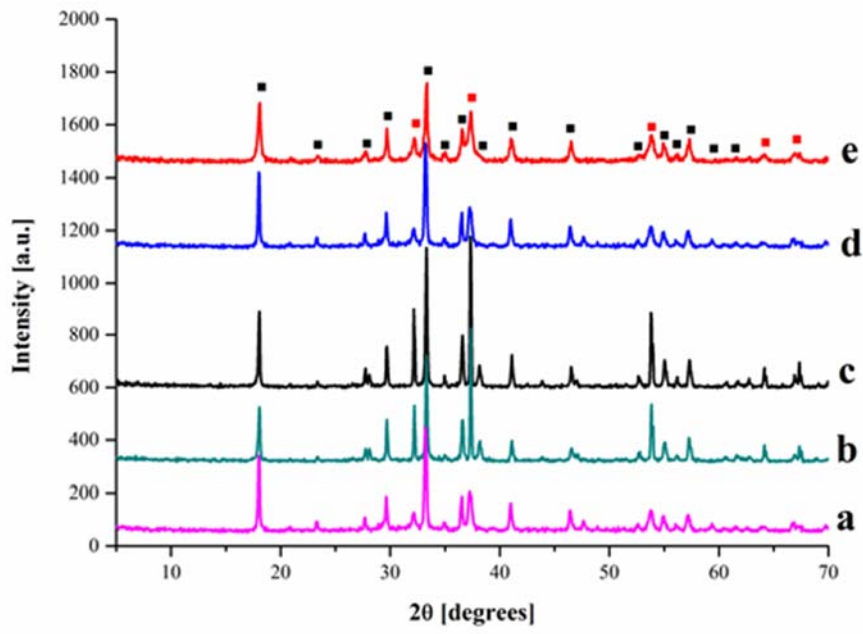


Figure 3.

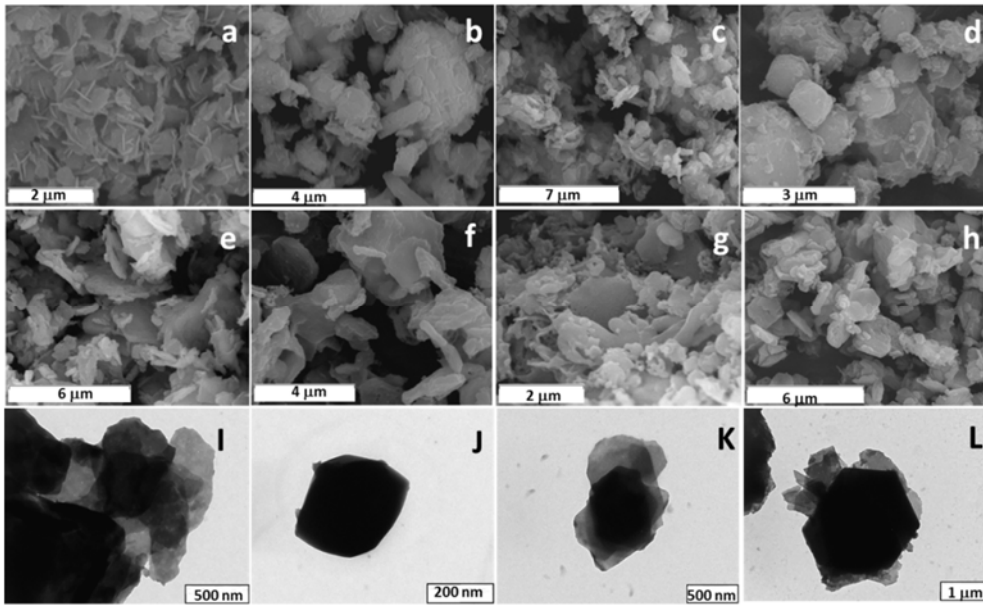


Figure 4.

■ Glycerol Conversion (%) ■ Selectivity to glycerol carbonate (%) ■ Selectivity to glycidol (%)

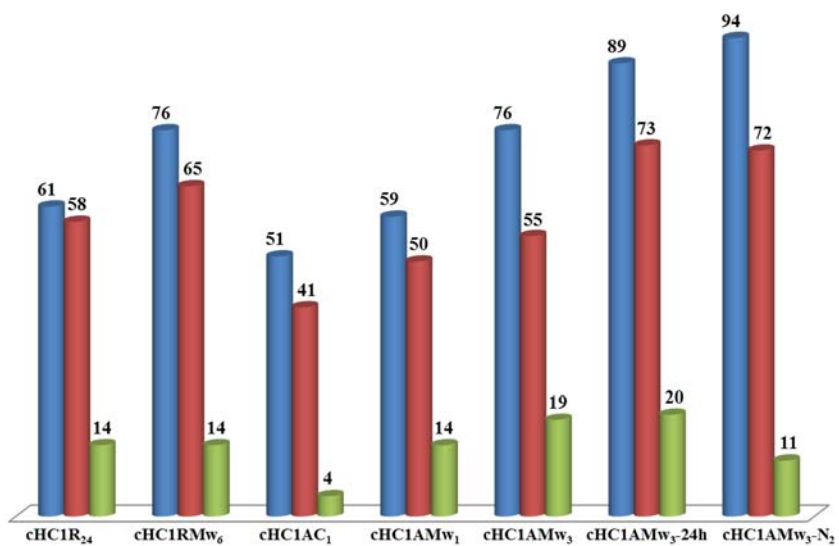


Figure 5.

■ Glycerol Conversion (%) ■ Selectivity to glycerol carbonate (%) ■ Selectivity to glycidol (%)

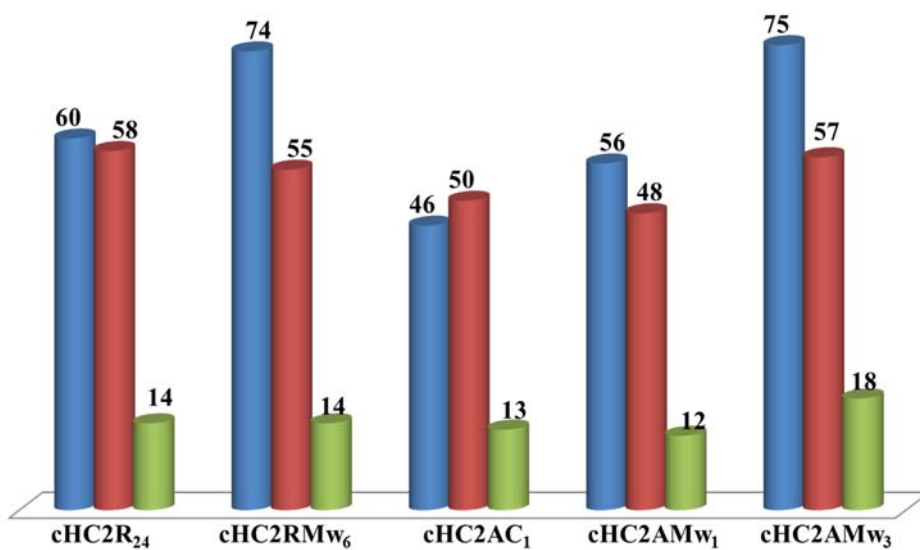


Figure 6.

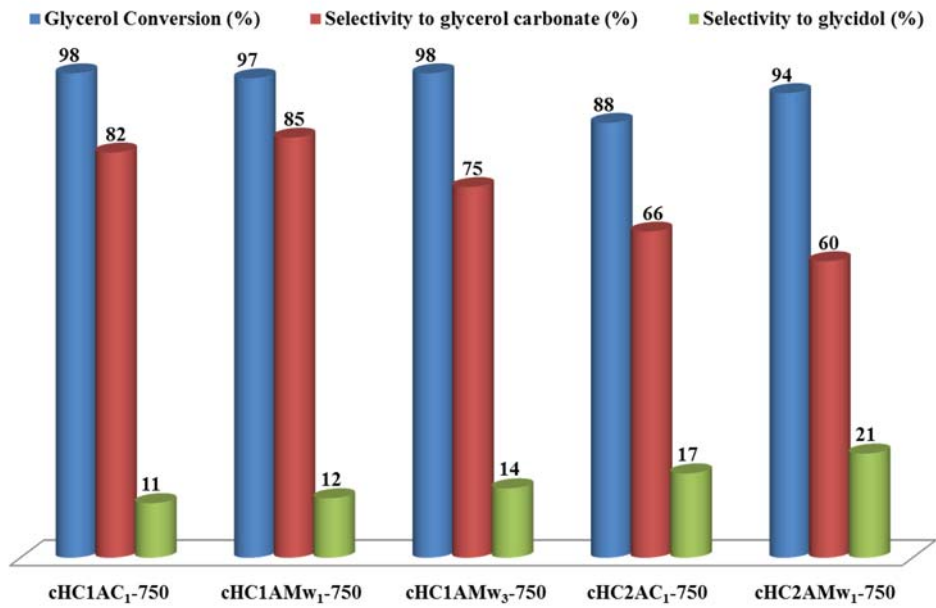


Figure 7.

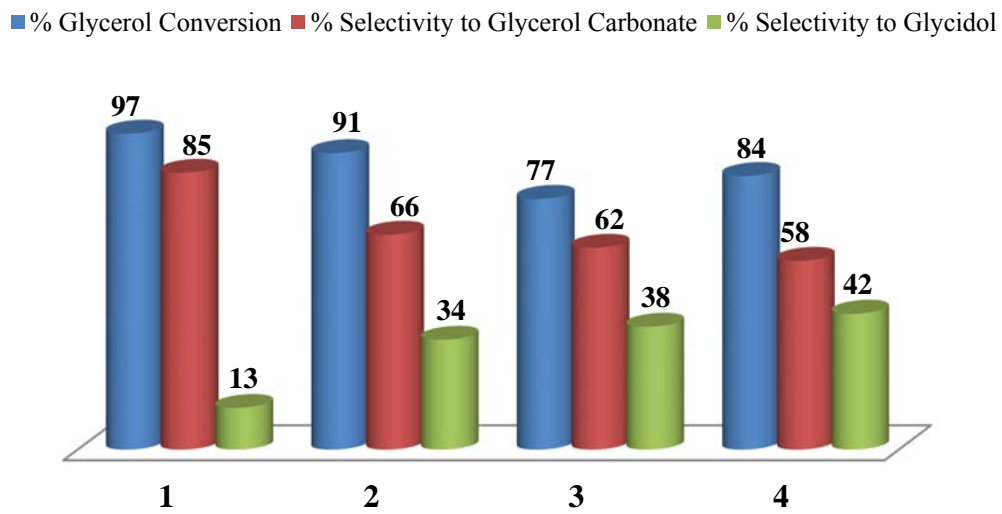


Figure 8.

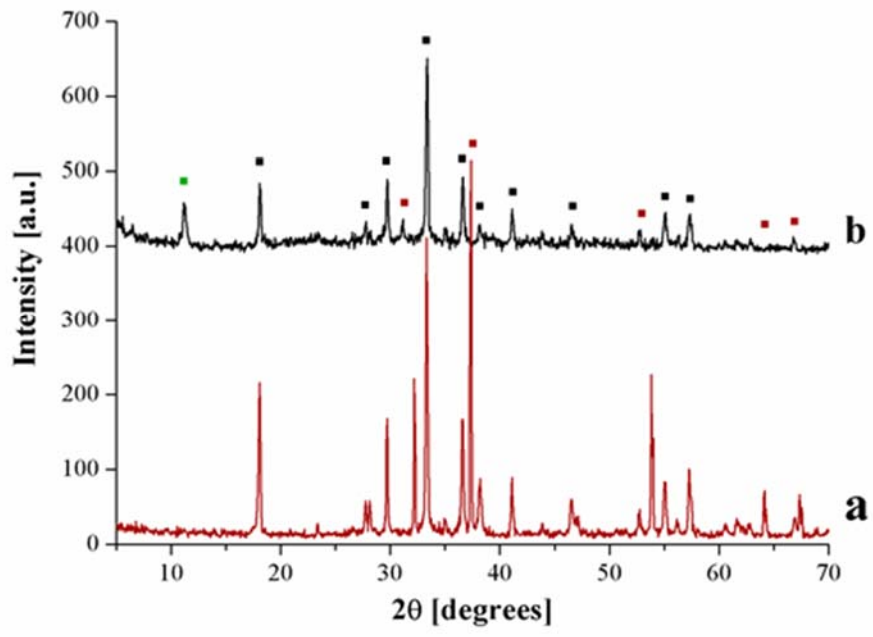


Figure 9.